Table of contents

Supplementary Figures

Supplementary Tables

Supplementary Figures

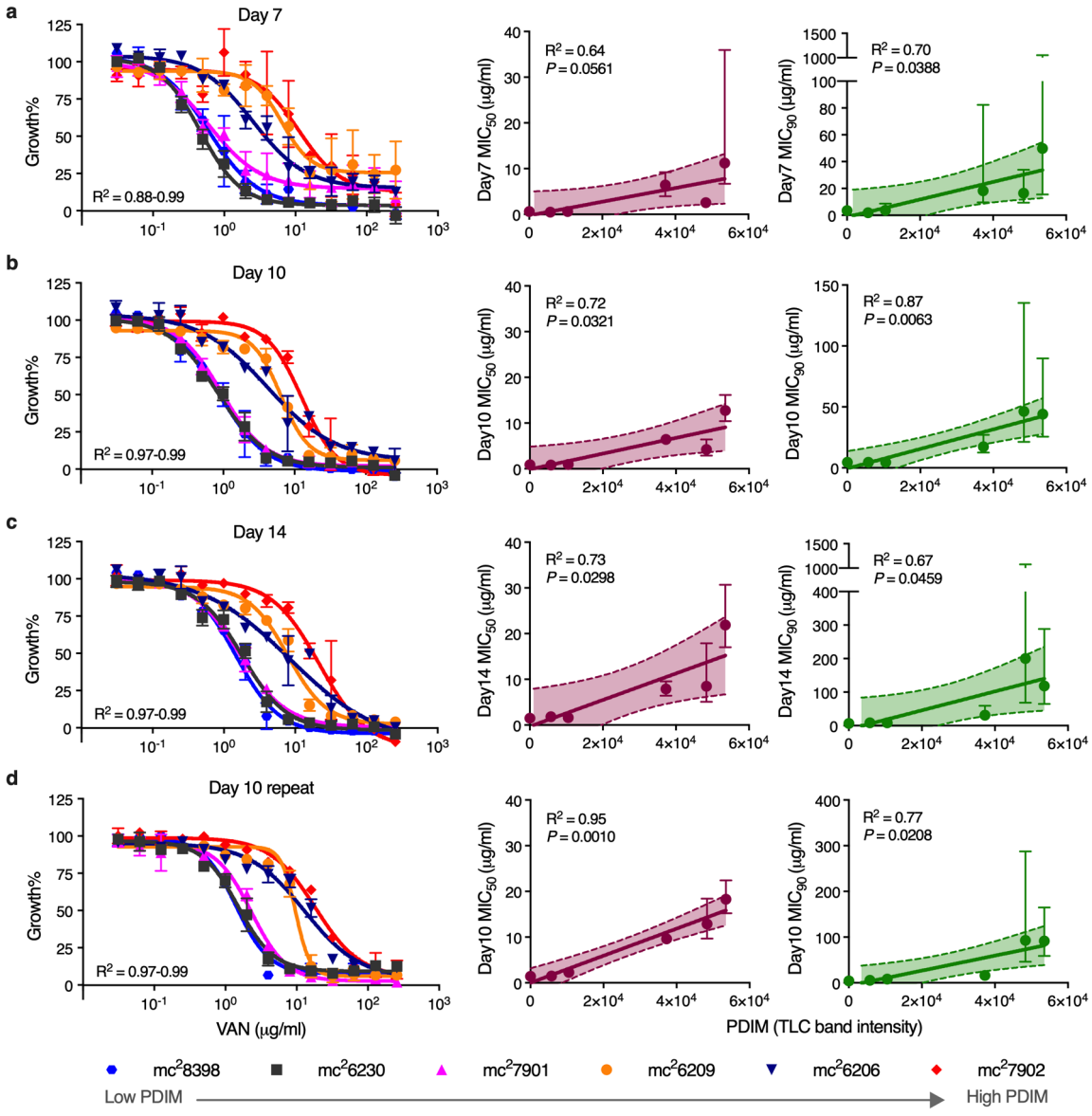

Supplementary Fig. 1 | Vancomycin resistance is predictive of PDIM production in *Mtb*. a–c, Vancomycin resistance of six BSL2-approved attenuated *Mtb* H37Rv strains (Supplementary Table 1) and correlation with PDIM lipid levels determined by TLC (Fig. 1a). These strains comprise our PDIM reference strain set. Minimum inhibitory concentration (MIC) assays were performed using the broth microdilution method in 7H9/OADC/glycerol/tyloxapol media with pantothenate, arginine, leucine, and methionine (PALM) supplements. Bacterial growth was measured after (**a**) 7, (**b**) 10, and (**c**) 14 days of incubation, and normalized to drug-free control wells. Simple linear regression was performed to assess the correlation between vancomycin MIC_{50} (maroon) and MIC_{90} (green) with PDIM levels as determined by TLC densitometric analysis of Fig. 1a. **d**, Experimental repeat measured after 10 days of incubation. MIC plots show mean ± SD for $n = 2$ biological replicates from a single experiment. Bands on regression plots show the 95% CI and error bars show the 95% CI for MIC values calculated from the curve fit.

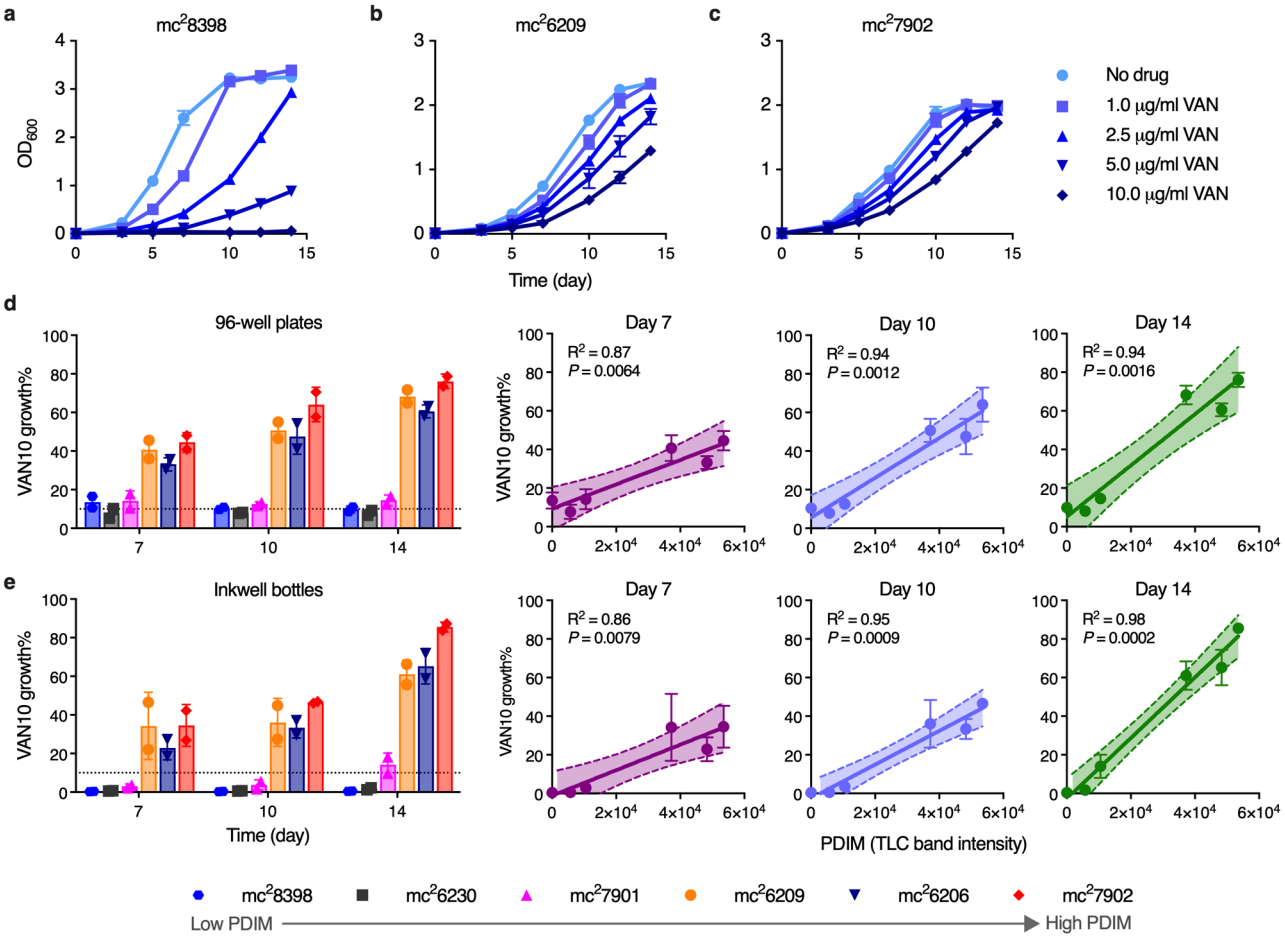

Supplementary Fig. 2 | VAN10 assay development. a–c, Growth curves of (**a**) *Mtb* mc²8398 [PDIM(-)], (**b**) mc²6209 [PDIM(+)], and (**c**) mc²7902 [PDIM(+)] (see Fig. 1a) in standard 7H9/OADC/glycerol/tyloxapol + PALM media with increasing concentrations of vancomycin. Mean ± SD for $n = 3$ biological replicates. For some data points the SD is smaller than the data symbols. This experiment was performed once. **d**,**e**, 'VAN10 assay' showing relative growth of the PDIM reference strain set in standard 7H9/OADC/glycerol/tyloxapol + PALM media with 10 μg/ml vancomycin compared to drug-free controls in (**d**) 96-well plates and (**e**) inkwell bottles. Bacterial growth was assessed by measuring optical density after 7, 10, and 14 days of incubation as indicated. VAN10 OD / VAN0 OD × 100 = VAN10 growth%. Simple linear regression was performed to assess the correlation between VAN10 growth% at each time point and PDIM lipid levels as determined by TLC densitometric analysis of Fig. 1a. Mean ± SD for $n = 2$ independent experiments, each performed in triplicate. The solid line indicates the linear regression best-fit, and the error bands the 95% CI.

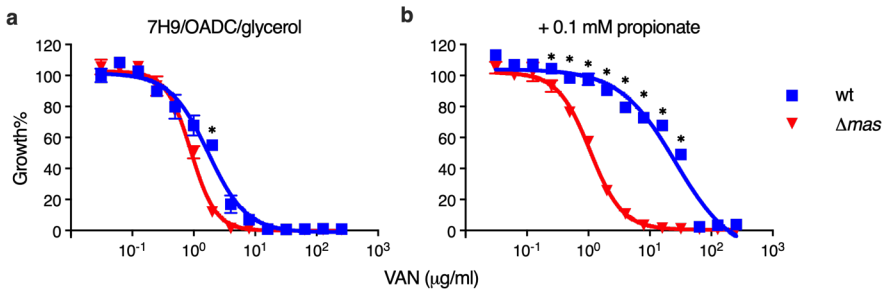

Supplementary Fig. 3 | VAN-P MIC assay validation in *Mtb* CDC1551. Vancomycin MIC assays of PDIM(+) (wildtype) and PDIM(-) (Δ*mas*) CDC1551 in **a**, standard 7H9/OADC/glycerol/tyloxapol media and **b**, supplemented with 0.1 mM propionate. Mean ± SD for $n = 2$ biological replicates from a single experiment. This experiment was performed once. $P < 0.001$; two-way ANOVA with Šidák's multiple comparison test. For some data points the SD is smaller than the data symbols.

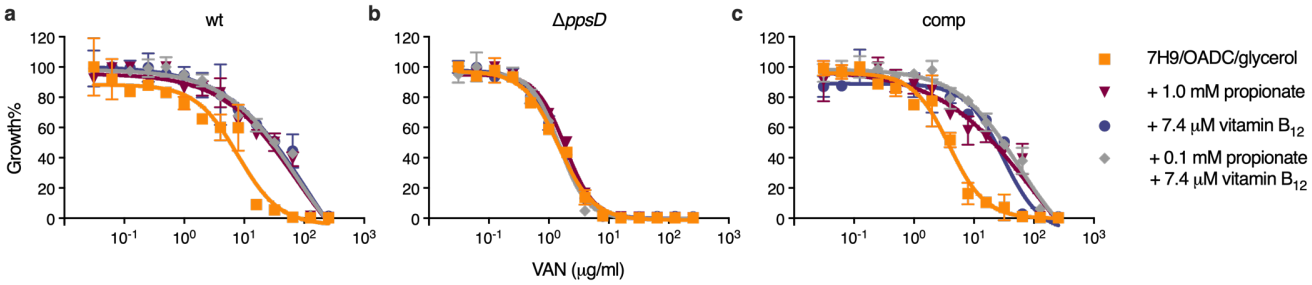

Supplementary Fig. 4 l Effect of propionate and vitamin B_{12} supplementation on vancomycin sensitivity of PDIM(+) and PDIM(-) *Mtb.* Vancomycin MIC assays of PDIM(+) and PDIM(-) *Mtb* H37Rv in standard 7H9/OADC/glycerol/tyloxapol media and supplemented with either 0.1 mM propionate or 7.4 μM vitamin B_{12} (10 μg/ml) alone and in combination. Mean ± SD for n = 2 biological replicates from a single experiment. For some data points the SD is smaller than the data symbols.

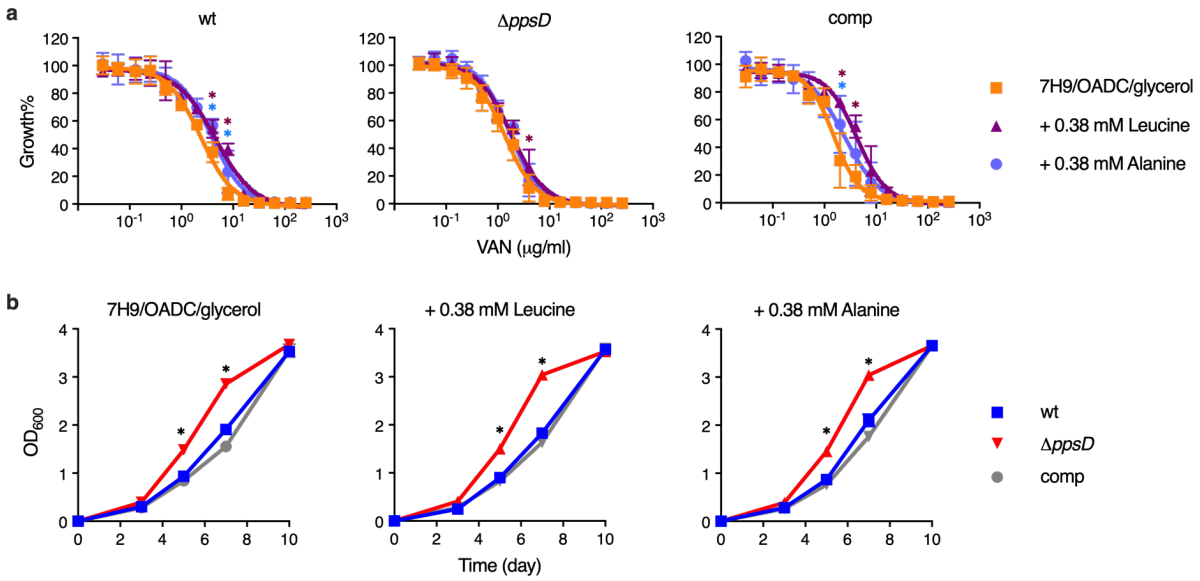

Supplementary Fig. 5 l Effect of leucine supplementation on vancomycin sensitivity and growth of PDIM(+) and PDIM(-) *Mtb*. a, Vancomycin MIC assays of PDIM(+) and PDIM(-) *Mtb* H37Rv in standard 7H9/OADC/glycerol/tyloxapol media and supplemented with either 0.38 mM L-leucine (50 mg/l, same concentration provided in PALM supplemented media) or 0.38 mM L-alanine as a non-branched-chain amino acid control. Mean ± SD for $n = 4$ biological replicates from two independent experiments. $P < 0.001$ compared to unsupplemented media; two-way ANOVA with Tukey's multiple comparison test. **b**, Growth of PDIM(+) and PDIM(-) H37Rv in standard 7H9/OADC/glycerol/tyloxapol media and supplemented with either L-leucine or L-alanine. Mean ± SD for $n = 3$ biological replicates. *$P < 0.001$ for both wt and comp versus Δ*ppsD*; two-way ANOVA with Tukey's multiple comparison test. This experiment was repeated once with similar results. For some data points the SD is smaller than the data symbols.

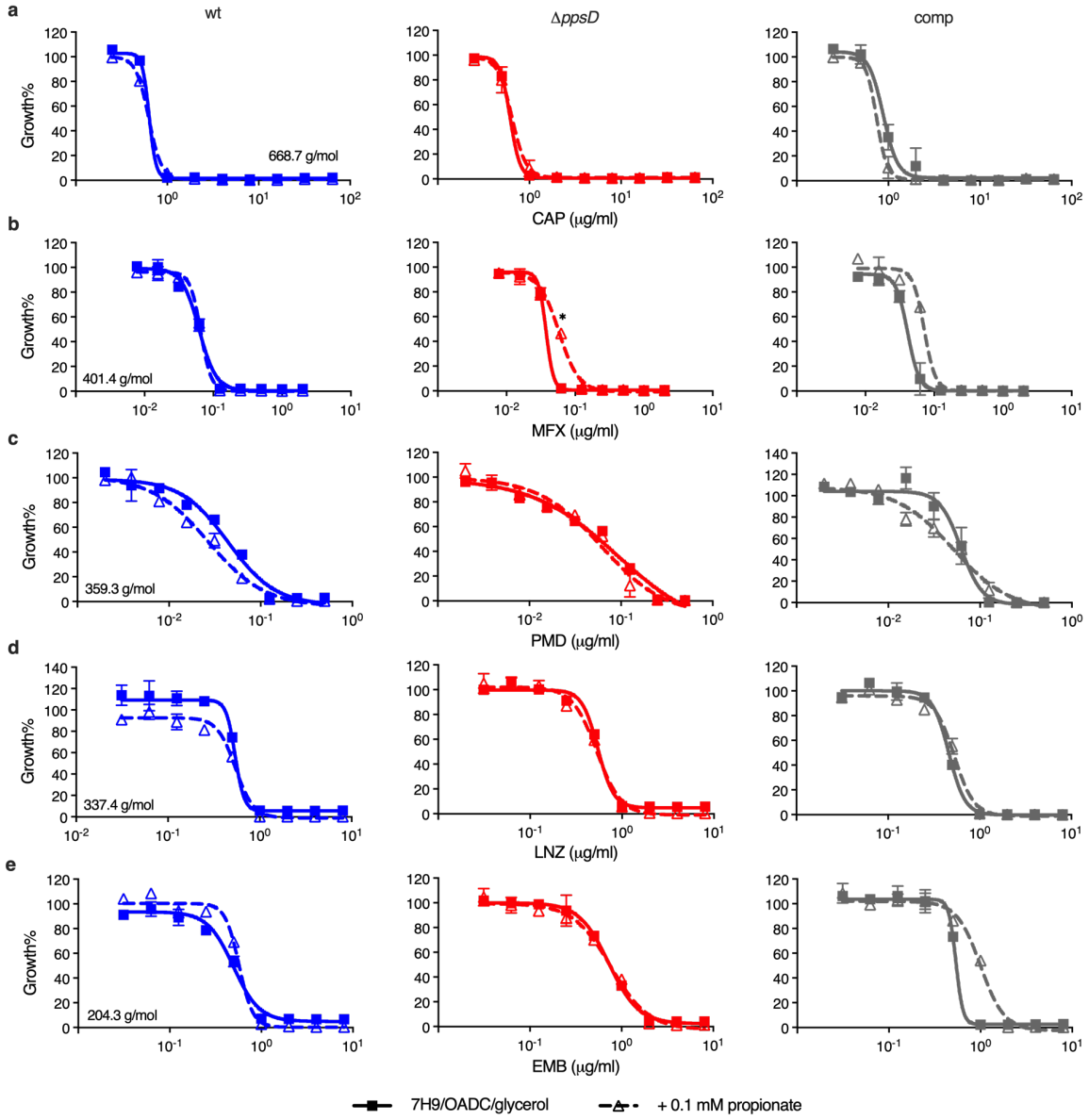

Supplementary Fig. 6 | Effect of propionate supplementation on the sensitivity of PDIM(+) and PDIM(-) *Mtb* to compounds with different modes of action and molecular weights. MIC assays of PDIM(+) and PDIM(-) *Mtb* H37Rv in 7H9/OADC/glycerol/tyloxapol media ± 0.1 mM propionate for **a**, capreomycin (CAP); **b**, moxifloxacin (MFX); **c**, pretomanid (PMD); **d**, linezolid (LNZ); and **e**, ethambutol (EMB). The molecular weight of each compound is shown on the corresponding MIC plot. Mean ± SD for $n = 2$ biological replicates from a single experiment. This experiment was performed once. For some data points the SD is smaller than the data symbols.

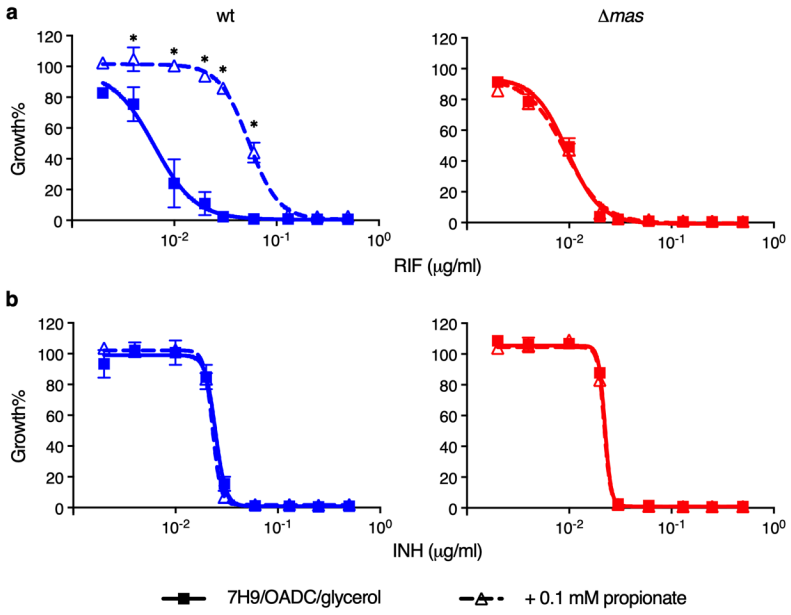

Supplementary Fig. 7 | Propionate increases the resistance of *Mtb* CDC1551 to rifampicin, but not isoniazid, in a PDIM-dependent manner. Sensitivity of PDIM(+) and PDIM(-) CDC1551 in 7H9/OADC/glycerol/tyloxapol media ± 0.1 mM propionate to **a**, rifampicin (RIF), and **b**, isoniazid (INH). Mean ± SD for $n = 2$ biological replicates from a single experiment. This experiment was performed once. *$P < 0.001$; two-way ANOVA with Šidák's multiple comparison test. For some data points the SD is smaller than the data symbols.

a

Metabolite	Abbreviation	*m/z* ([M-H]$^-$)	R/T (min)	Comment
Pyruvate	PYR	87.0088	2.7	
Succinate	SUC	117.0193	11.7	
2-methyl(iso)citrate	2M(I)C	205.0354	10.4	Poorly resolved. Not detected in samples.
Propionyl-CoA	PROP-CoA	822.1341	14.0	
Succinyl-CoA	SUC-CoA	866.1240	19.5	Not detected in samples.
Methylmalonyl-CoA	MMCoA	866.1240	21.2	

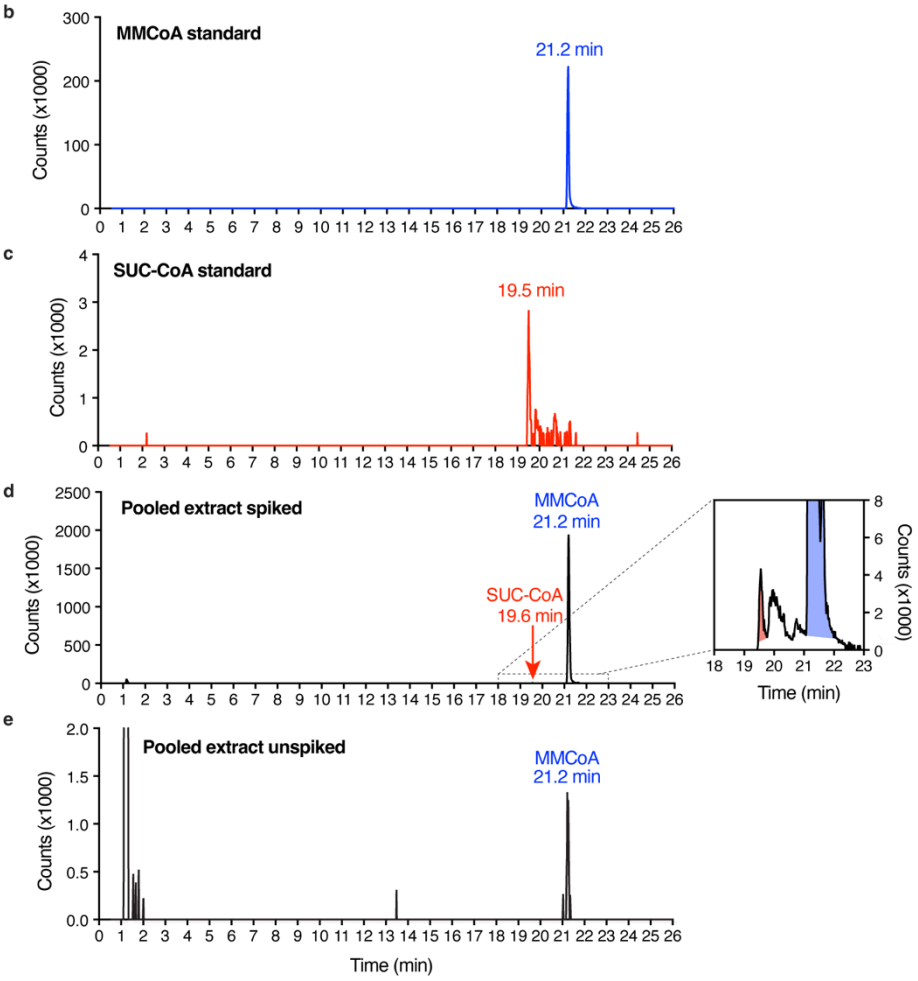

Supplementary Fig. 8 | LC-MS *m/z* values, retention times, and separation of methylmalonyl-CoA and succinyl-CoA. **a**, Chromatographic retention times (R/T) and *m/z* values for metabolites in methylmalonyl-CoA production and propionyl-CoA catabolism. **b-e.** Chromatographic separation of methylmalonyl-CoA and succinyl-CoA. Extracted ion chromatograms (*m/z* 866.1240) for (**b**) methylmalonyl-CoA and (**c**) succinyl-CoA standards alone (25 μM), (**d**) pooled mycobacterial extract spiked with a standard mixture (100 μM), and (**e**) and the same extract unspiked.

Supplementary Tables

Supplementary Table 1 | BSL2-approved attenuated *Mtb* strains included in this study. These strains comprise our PDIM reference strain set, with the exception of mc²6230 AE1601 and AE1611, which are PDIM(+) and PDIM(-) clones isolated from our mc²6230 stock.

Strain name	Genotype	Reference
mc²6206	H37Rv Δ*panCD* Δ*leuCD*	Jain *et al.* (2014)[29]
mc²6209	H37Rv Δ*panCD* Δ*leuCD* Δ*secA2*	Jain *et al.* (2014)[29]
mc²6230	H37Rv ΔRD1 Δ*panCD*	Sambandamurthy *et al.* (2006)[68]; Jain *et al.* (2012)[69]
mc²7901	H37Rv Δ*panCD* Δ*leuCD* Δ*metA*	Vilchèze *et al.* (2018)[70]
mc²7902	H37Rv Δ*panCD* Δ*leuCD* Δ*argB*	Vilchèze *et al.* (2018)[70]
mc²8398	H37Rv Δ*metA* Δ*argB*	Jacobs and Tiwari (2023)[71]
mc²6230 AE1601*	H37Rv ΔRD1 Δ*panCD* [PDIM(+)]	This study
mc²6230 AE1611†	H37Rv ΔRD1 Δ*panCD* [PDIM(-)]	This study

*PDIM(+) and †PDIM(-) clones identified by VAN10-P screening of single colonies (see also Extended Data Fig. 4j and Supplementary Table 3).

Supplementary Table 2 | Virulent *Mtb* strains included in this study. Single PDIM(+) clones isolated in this study have been assigned unique 'AE' reference numbers as indicated.

Strain name	Genotype	Source/Construction
H37Rv-A	H37Rv	In-house culture collection
H37Rv-B	H37Rv	C57BL/6 mouse passage of H37Rv-A
H37Rv-SC (AE1028)*	H37Rv	PDIM(+) clone isolated from H37Rv-B
H37Rv Δ*ppsD*	H37Rv Δ*Rv2934* hyg^R	Specialized transduction of H37Rv-SC
H37Rv Δ*ppsD*::comp	H37Rv Δ*Rv2934*::comp hyg^R kan^R	Transformation of H37Rv Δ*ppsD* with pMV361-*ppsD*
H37Rv Δ*tgs1*-1	H37Rv Δ*Rv3130c* hyg^R	Specialized transduction of H37Rv-B
H37Rv Δ*tgs1*-2	H37Rv Δ*Rv3130c* hyg^R	Specialized transduction of H37Rv-B
H37Rv Δ*tgs1*-3	H37Rv Δ*Rv3130c* hyg^R	Specialized transduction of H37Rv-B
H37Rv Δ*tgs1*-4	H37Rv Δ*Rv3130c* hyg^R	Specialized transduction of H37Rv-B
H37Rv Δ*tgs1*-5	H37Rv Δ*Rv3130c* hyg^R	Specialized transduction of H37Rv-B
H37Rv Δ*tgs1*-7	H37Rv Δ*Rv3130c* hyg^R	Specialized transduction of H37Rv-B
H37Rv Δ*tgs1*-8	H37Rv Δ*Rv3130c* hyg^R	Specialized transduction of H37Rv-B
H37Rv Δ*tgs1*-9	H37Rv Δ*Rv3130c* hyg^R	Specialized transduction of H37Rv-B
CDC1551-A	CDC1551	In-house culture collection
CDC1551-B	CDC1551	In-house culture collection
CDC1551 Δ*mas*	CDC1551 Δ*Rv2940c* hyg^R	Specialized transduction of CDC1551-B
Erdman	Erdman	In-house culture collection
HN878	HN878	In-house culture collection
KZN 4207	KZN 4207	In-house culture collection
CDC1551-SC (AE5005)*	CDC1551	PDIM(+) clone isolated from a Rag-/- mouse
Erdman-SC (AE3003)*	Erdman	PDIM(+) clone isolated from a Rag-/- mouse
HN878-SC (AE8005)*	HN878	PDIM(+) clone isolated from a Rag-/- mouse

*PDIM(+) clone identified by VAN10-P screening of single colonies (see also Extended Data Fig. 4 and Supplementary Table 3).

Supplementary Table 3 | PDIM mutations in *Mtb* strains included in this study. Non-synonymous variants in genes involved in PDIM biosynthesis, assembly, processing, or transport (see Fig. 2e). Mutations are described at the protein level for amino acid substitutions (p.) and at the gene coding level for frameshift/INDEL mutations (c.). Variants were identified from Illumina MiSeq WGS data using the software tool Pilon[66] for variant calling unless indicated. We note the Erdman reference sequence contains a frameshift mutation that disrupts the *ppsA* gene [c.2858(C)$_{6\to5}$]. Both our Erdman strains lack this mutation and have an intact *ppsA* gene. For mutations with mixed coverage (< 90%) the frequency of the variant allele is given in brackets. 'H37Rv-B col#' are single colonies isolated from H37Rv-B with different VAN10-P growth%, including a subset of those that had an intermediate VAN10-P phenotype (see Fig. 2d). '≥ 10 ×' is the percentage of genome with 10 × or greater coverage.

Strain	Genome coverage (×)			PDIM mutations
	Mean	SD	≥ 10 ×	
mc²6206	66.3	17.4	99.00%	n.d.
mc²6209	56.8	21.8	98.90%	n.d.
mc²6230	187.0	73.8	98.50%	*ppsC* c.2685(C)$_{7\to8}$ (66%)†
mc²6230 AE1601*	171.7	32.6	99.11%	n.d.
mc²6230 AE1611	30.5	9.4	97.26%	*ppsC* c.2685(C)$_{7\to8}$ ‡
mc²7901	26.7	10.5	96.50%	*fadD28* p.Arg562Gly
mc²7902	47.8	15.9	98.50%	n.d.
mc²8398	62.1	16.7	99.20%	*ppsC* c.2475delC
H37Rv-A	93.5	31.0	97.60%	n.d.
H37Rv-B	60.5	18.3	97.80%	n.d.
H37Rv-SC (AE1028)*	57.1	19.6	98.90%	n.d.
H37Rv Δ*ppsD*	58.7	18.6	98.70%	Δ*ppsD*
H37Rv Δ*tgs1*-1	95.6	56.5	91.70%	*fadD28* p.Leu241Pro
H37Rv Δ*tgs1*-2	90.3	78.6	83.00%	*ppsA* p.Trp968*
H37Rv Δ*tgs1*-3	17.2	7.0	87.20%	*ppsD* p.Ser247Pro
H37Rv Δ*tgs1*-4	86.3	25.1	97.70%	*ppsE* p.Asp74Asn
H37Rv Δ*tgs1*-5	119.4	57.2	96.50%	*ppsC* c.2668(C)$_{7\to6}$ ‡
H37Rv Δ*tgs1*-7	184.5	138.4	93.10%	n.d.
H37Rv Δ*tgs1*-8	58.2	15.1	99.00%	*ppsC* c.2668(C)$_{7\to8}$ ‡
H37Rv Δ*tgs1*-9	69.7	18.0	99.10%	*ppsC* c.2668(C)$_{7\to6}$ ‡
CDC1551-A	106.5	49.8	96.90%	n.d.
CDC1551-B	54.7	19.6	98.80%	n.d.
CDC1551 Δ*mas*	44.0	18.6	96.50%	Δ*mas*
Erdman	84.7	25.2	98.00%	*ppsA* c.3418insA (72%)
HN878	76.1	44.3	93.10%	n.d.
KZN 4207	86.7	38.1	97.10%	n.d.
CDC1551-SC (AE5005)*	69.3	18.9	99.10%	n.d.
Erdman-SC (AE3003)*	91.2	23.5	99.30%	n.d.
HN878-SC (AE8005)*	65.9	24.4	97.90%	n.d.
H37Rv-B col5 (VAN10-P 41%)	61.0	15.7	99.00%	*ppsE* p.Asp74Asn
H37Rv-B col6 (VAN10-P 1%)	53.9	14.8	98.70%	*ppsA* p.Trp968*
H37Rv-B col16 (VAN10-P 43%)	50.7	13.7	98.60%	*ppsE* p.Asp74Asn
H37Rv-B col17 (VAN10-P 77%)	34.9	13.0	97.90%	n.d.
H37Rv-B col19 (VAN10-P 31%)	94.0	25.0	99.10%	*ppsE* p.Asp74Asn
H37Rv-B col23 (VAN10-P 39%)	38.2	11.2	98.10%	*ppsE* p.Asp74Asn
H37Rv-B col36 (VAN10-P 1%)	62.9	15.7	98.90%	*ppsA* p.Trp968*

*PDIM(+) clone identified by VAN10-P screening of single colonies (see also Extended data Fig. 4).

†Mutation identified using the Illumina NextSeq platform (see also Supplementary Table 5).

‡Mutation detected/confirmed by PCR and Sanger sequencing (see also Extended data Fig. 5).

n.d. = no non-synonymous PDIM mutations detected.

Supplementary Table 4 | Low-frequency PDIM mutation analysis. Low-frequency non-synonymous PDIM mutations detected in laboratory stocks of virulent *Mtb* strains (See Fig. 2a). Mutations are described at the protein level for amino acid substitutions (p.) and at the gene coding level for frameshift/INDEL mutations. Variant calling was performed using the Geneious variant finder with the following thresholds: ≥ 10% variant frequency, ≥ 10 × coverage, $P < 1 \times 10^{-10}$.

Strain	PDIM mutations	Frequency	REF/ALT	*P* value
H37Rv-A	*ppsB* p.Leu250Pro	11.6%	99/13	3.1×10^{-23}
H37Rv-B	n.d.			
Erdman	*ppsA* c.3418insA	67.9%	27/57	2.9×10^{-161}
	ppsE p.Cys414*	10.7%	50/6	3.2×10^{-14}
KZN 4207	n.d.			
HN878	*fadD28* c.347delT	14.3%	126/21	2.6×10^{-30}
	ppsD p.Gly1636Arg	18.8%	26/6	1.4×10^{-14}
CDC1551-A	*ppsA* p.Phe327Val	10.2%	115/13	7.1×10^{-20}
	ppsE c.3496insA	12.6%	118/17	9.9×10^{-41}
CDC1551-B	n.d.			

n.d. = no non-synonymous PDIM mutations detected.

Supplementary Table 5 | Identification of an unfixed *ppsC* frameshift mutation in mc²6230 by Illumina NextSeq. VAN-P assays and TLC lipid analysis determined mc²6230 is highly PDIM deficient (Fig. 1a,c,e), however, WGS by Illumina MiSeq failed to identify any PDIM mutations in this strain and we subsequently established our mc²6230 stock is a mixed population (Extended Data Fig. 4h). Resequencing using the Illumina NextSeq platform identified an unfixed frameshift mutation in *ppsC* [c.2685(C)$_{7\rightarrow8}$] that was not detected by Illumina MiSeq due to poor coverage over this region. To assess the relationship between overall coverage and coverage over the homopolymeric region NextSeq reads were randomly downsampled. The number following 'NextSeq_' represents the fraction of reads sampled (i.e. 0.8 = 80% of reads retained).

Genome	Genome coverage (×)			HT region (×)[a]		AF[b]
	mean	s.d.	≥ 10 ×	mean	s.d.	
mc²6230 MiSeq	187.0	73.8	98.5%	0.6	0.00	0%
mc²6230 NextSeq	124.5	23.5	99.2%	32.0	0.13	66%
mc²6230 NextSeq_0.8	103.6	20.1	99.1%	27.2	0.13	63%
mc²6230 NextSeq_0.6	81.0	16.5	99.0%	19.1	0.12	58%
mc²6230 NextSeq_0.4	56.4	12.4	98.8%	19.6	0.14	68%
mc²6230 NextSeq_0.2	29.6	7.7	98.2%	5.5	0.16	80%

[a] Read depth over the *ppsC* homopolymeric tract region (3258352-3258375) (See also Extended Data Fig. 5a).

[b] Allele frequency of the *ppsC* c.2685(C)$_{7\rightarrow8}$ frameshift mutation.

Supplementary Table 6 | Culture media reagents and supplements used in this study.

Name	Catalog #	Supplier
Middlebrook 7H9	271310	BD Difco
Middlebrook 7H10	262710	BD Difco
Glycerol	G33	Fisher Chemical
Dextrose (D-glucose)	D16	Fisher Chemical
Tyloxapol	T8761	Sigma-Aldrich
Tween 80	P1754	Sigma-Aldrich
Sodium oleate	11-1280	Strem Chemicals
Bovine serum albumin fraction V	A-420-1	GoldBio
Catalase	C1345	Sigma-Aldrich
D-Calcium pantothenate	243305000	Acros Organics
L-Arginine	A5006	Sigma-Aldrich
L-Leucine	L8000	Sigma-Aldrich
L-Methionine	166165000	Acros Organics
Hygromycin B	10687010	Invitrogen
Kanamycin	BP906	Fisher BioReagents
Sodium propionate	P1880	Sigma-Aldrich
Vitamin B_{12}	V2876	Sigma-Aldrich
Sodium pyruvate	BP356	Fisher BioReagents
Sodium acetate	A13184.30	Thermo Scientific Chemicals
Sodium butyrate	A11079.06	Thermo Scientific Chemicals
Valeric acid	149570050	Acros Organics
Cholesterol	C3045	Sigma-Aldrich

Supplementary Table 7 | Primers used in this study.

Primer name	Sequence
ppsC homopolymeric tract region	
ppsC_homopoly_F	CTGCTGACCCACTCGATCA
ppsC_homopoly_R	TGTCGGGCCTGTGGTAAG
Knockout strain confirmation	
Universal_uptag	GATGTCTCACTGAGGTCTCT
Rv2940c_LL	TCATGGGCATCACGTTAC
Rv2940c_LR	AGAACTCAGCATCGAAACC
Rv2934_LL	CATGCAGGCGGTACTCAC
Rv2934_LR	GGATCGGGATCGTAGAAC
Rv3130c_LL	CACAATGGCTTTCATTCG
Rv3130c_LL	GGGTACAGGGACGTAGGC
pMV361-*ppsD* vector construction and confirmation	
pMV361_ppsD_Hsp60_for	GATCCAGCTGCAGAATTCATGACAAGTCTGGCGGAGCG
pMV361_ppsD_rev	CTACGTCGACATCGATAAGCTTCTTATCCTCCCTGTACTTCAGGTTTAGGT
pMV361_vector_for	GAATTCTGCAGCTGGATCCGC
complement_vector_rev	GAAGCTTATCGATGTCGACGTAG
pMV361-LL	GGAATCACTTCGCAATGGC
pMV361-LR	ATCGTACGCTAGTTAACTACG
ppsD_sequencing_2	CGCCAGCGCTCGCAAC
ppsD_sequencing_3	CGGTGCTGGCCGACTGGATG
ppsD_sequencing_4	GGCATAAAAATCGGCCGGCG
ppsD_sequencing_5	TAATTCGCGGCGGGGACAGC
ppsD_sequencing_6	CGAAGCGGCGGAAGAGAATCC
ppsD_sequencing_7	TCTGGGGGCCAATTGCGCGG

Supplementary Table 8 | Inhibitors used in this study.

Name	Abbreviation	Catalog #	Supplier
Azithromycin dihydrate	AZM	A2076	TCI America
Bedaquiline	BDQ	Gift	Kevin Pethe, Nanyang Technological University, Singapore
Capreomycin sulfate	CAP	J66684	Alfa Aesar
Ethambutol dihydrochloride	EMB	J60695	Alfa Aesar
Erythromycin	ERY	E0751	TCI America
Isoniazid	INH	I3377	Sigma
Linezolid	LNZ	460592500	Acros Organics
Moxifloxacin hydrochloride	MFX	457960010	Acros Organics
Pretomanid	PMD	HY-10844	MedChemExpress
Ramoplanin	RAM	sc-253424	Santa Cruz Biotechnology
Rifampicin	RIF	R3501	Sigma
Teicoplanin (A2)	TEC	RS048	BIOTANG Inc.
Vancomycin hydrochloride	VAN	J62790	Alfa Aesar

Supplementary Table 9 | Chemical standards used for LC-MS.

Name	Catalog #	Supplier
2-Methylcitric Acid	29327	Cayman Chemical
n-Propionyl coenzyme A lithium salt	P5397	Sigma-Aldrich
Methylmalonyl coenzyme A tetralithium salt	sc-215385	ChemCruz
Succinic acid	33272	Alfa Aesar
Succinyl-Coenzyme A (sodium salt)	23297	Cayman Chemical
Sodium pyruvate	BP356	Fisher BioReagents

Supplementary Table 10 | Putative metabolites used for LC-MS data normalization.

Compound	m/z [(M-H)$^-$]	Pathway
Glycine	74.0248	Amino acids and amino acid metabolism
Pyruvic acid	87.0088	Central carbon
L-Alanine	88.0404	Amino acids and amino acid metabolism
L-Serine	104.0353	Amino acids and amino acid metabolism
Uracil	111.0200	Nucleotide metabolism
L-Proline	114.0561	Amino acids and amino acid metabolism
L-Valine	116.0717	Amino acids and amino acid metabolism
Succinic acid	117.0193	Central carbon
L-Threonine	118.0510	Amino acids and amino acid metabolism
Nicotinic acid	122.0248	Nicotinate and nicotinamide metabolism
L-Leucine	130.0874	Amino acids and amino acid metabolism
L-Isoleucine	130.0874	Amino acids and amino acid metabolism
L-Aspartic Acid	132.0302	Amino acids and amino acid metabolism
L-Malic acid	133.0142	Central carbon
Adenine	134.0472	Nucleotide metabolism
Salicylic acid	137.0244	Other
4-Hydroxybenzoic acid	137.0244	Folate biosynthesis
alpha-Ketoglutaric acid	145.0142	Central carbon
L-Glutamine	145.0619	Amino acids and amino acid metabolism
L-Lysine	145.0983	Amino acids and amino acid metabolism
L-Glutamic acid	146.0459	Amino acids and amino acid metabolism
L-Methionine	148.0438	Amino acids and amino acid metabolism
Guanine	150.0421	Nucleotide metabolism
L-Histidine	154.0622	Amino acids and amino acid metabolism
Orotic acid	155.0098	Nucleotide metabolism
L-Phenylalanine	164.0717	Amino acids and amino acid metabolism
DL-Glyceraldehyde 3-phosphate	168.9907	Central carbon
Dihydroxyacetone phosphate	168.9907	Central carbon
D-Glycerol 3-phosphate	171.0064	Central carbon
Shikimic acid	173.0455	Amino acids and amino acid metabolism
N2-Acetyl-L-ornithine	173.0932	Amino acids and amino acid metabolism
L-Arginine	173.1044	Amino acids and amino acid metabolism
a-D-Glucose	179.0561	Central carbon
L-Tyrosine	180.0666	Amino acids and amino acid metabolism
L-Tryptophan	203.0826	Amino acids and amino acid metabolism
Thymidine	241.0830	Nucleotide metabolism
D-Fructose 6-P/a-D-Glucose 6-P	259.0224	Central carbon
Adenosine	266.0895	Nucleotide metabolism
Inosine	267.0735	Nucleotide metabolism
dTMP	321.0493	Nucleotide metabolism
cAMP	328.0452	Nucleotide metabolism
Trehalose/Maltose	341.1089	Central carbon
5'-AMP	346.0558	Nucleotide metabolism
dTDP	401.0157	Nucleotide metabolism
Trehalose 6-phosphate	421.0753	Central carbon
ADP	426.0221	Nucleotide metabolism
ATP	505.9885	Nucleotide metabolism
Acetyl-CoA	808.1185	Central carbon
Propionyl-CoA	822.1341	Central carbon
Methylmalonyl-CoA	866.1240	Central carbon

Supplementary Table 11 | Whole genome sequencing accession numbers. BioProject PRJNA923717.

Strain	BioSample accession	SRA accession number/s		
mc²6206	SAMN32734011	SRR23080350		
mc²6209	SAMN32734012	SRR23080349		
mc²6230	SAMN32734013	SRR23080327	SRR23080338*	SRR23080318†
mc²6230 AE1601	SAMN35027541	SRR24495990†		
mc²6230 AE1611	SAMN35027542	SRR24495989		
mc²7901	SAMN32734014	SRR23080317		
mc²7902	SAMN32734015	SRR23080316		
mc²8398	SAMN32734016	SRR23080315		
H37Rv-A	SAMN32734017	SRR23080314		
H37Rv-B	SAMN32734018	SRR23080313		
H37Rv-SC (AE1028)	SAMN32734019	SRR23080348		
H37Rv Δ*ppsD*	SAMN32734020	SRR23080347		
H37Rv Δ*tgs1*-1	SAMN32734021	SRR23080346		
H37Rv Δ*tgs1*-2	SAMN32734022	SRR23080345		
H37Rv Δ*tgs1*-3	SAMN32734023	SRR23080344		
H37Rv Δ*tgs1*-4	SAMN32734024	SRR23080343		
H37Rv Δ*tgs1*-5	SAMN32734025	SRR23080342	SRR23080341*	
H37Rv Δ*tgs1*-7	SAMN32734026	SRR23080340	SRR23080339*	
H37Rv Δ*tgs1*-8	SAMN32734027	SRR23080337		
H37Rv Δ*tgs1*-9	SAMN32734028	SRR23080336		
CDC1551-A	SAMN32734029	SRR23080335		
CDC1551-B	SAMN32734030	SRR23080334		
CDC1551 Δ*mas*	SAMN32734031	SRR23080333*		
Erdman	SAMN32734032	SRR23080332		
HN878	SAMN32734033	SRR23080331		
KZN 4207	SAMN32734034	SRR23080330		
CDC1551-SC (AE5005)	SAMN32734035	SRR23080329		
Erdman-SC (AE3003)	SAMN32734036	SRR23080328		
HN878-SC (AE8005)	SAMN32734037	SRR23080326		
H37Rv-B col5	SAMN32734038	SRR23080325		
H37Rv-B col6	SAMN32734039	SRR23080324		
H37Rv-B col16	SAMN32734040	SRR23080323		
H37Rv-B col17	SAMN32734041	SRR23080322		
H37Rv-B col19	SAMN32734042	SRR23080321		
H37Rv-B col23	SAMN32734043	SRR23080320		
H37Rv-B col36	SAMN32734044	SRR23080319		

*Data acquired using Illumina MiSeq with a 300-cycle kit (76 bp reads). †Data acquired on the Illumina NextSeq system (151 bp reads). All remaining data was acquired using Illumina MiSeq with a 600-cycle kit (301 bp reads).